# Theoretical pressure and friction in total disc prosthesis for lumbar spine. Influence of ball radius and biomaterial combination

I. ROTARU[a,b,*], D. OLARU[a]
[a]*Department of Mechanical Engineering, Mechatronics and Robotics, Faculty of Mechanical Engineering, "Gheorghe Asachi" Technical University of Iasi, 61-63 Bd. Dimitrie Mangeron, 700050 Iasi, Romania*
[b] *Department of Biomedical Sciences, Faculty of Medical Bioengineering, "Gr.T.Popa" University of Medicine and Pharmacy of Iasi, 9-13M. Kogalniceanu Street, 700454 Iasi, Romania*

Total disc prosthesis for lumbar spine is a medical device used to completely replace the damaged intervertebral lumbar disc. The main advantages of prosthesis implantation are that this conserves the intervertebral mobility and prevents the adjacent discs degeneration. The purpose of this work was to study the theoretical effect of ball radius on the maximum pressure and on the frictional torque which occurs within lumbar total disc prostheses made of different biomaterial combination. The design of total disc prosthesis investigated was ball-and-socket and the biomaterial couple was metal-on-metal, polymer-on-metal and ceramic-on-ceramic. The results of this study indicated that the maximum pressure in disc prosthesis decrease with ball radius, while the frictional torque has a linear increase with ball radius. This study suggested designing of total disc prostheses for lumbar spine with small ball radius and with ceramic-on-ceramic material combination.

(Received April 20, 2013; accepted May 7, 2015)

*Keywords*: Ball-and-Socket, Biomaterial, Friction, Pressure, Disc Prosthesis

## 1. Introduction

Nowadays the degenerative disc disease on lumbar spine has a high frequency and this could cause low back pain or even lumbar disc herniation. The gold standard in treatment of a herniated disc is represented by the spinal fusion procedure using metal or composite cages [1,2]. In recent years the implantation of total disc prosthesis has been introduced as an alternative method to this procedure [3-9].

Total disc prostheses are medical devices which keep the intervertebral mobility, prevent the degeneration of adjacent intervertebral discs [3-6] and consist of two or three functional components: there are always two endplates and the relative movements are determined by a prosthetic nucleus which is either separated or connected to the inferior endplate [7-14].

The first described total disc prosthesis was the Fernstorm's steel-ball endoprosthesis in 1966. The first commercially distributed prosthesis was introduced in 1982 by Schellnack and Buttner-Janz [5-9]. Since then, several prosthetic designs have been proposed such as synthetic intervertebral disc composed of hydroxyapatite endplates and reinforced hydrogels [15,16].

The currently used total artificial discs can be categorized based on their bearing surfaces as metal-on-metal (e.g. Maverick, FlexiCore, Kineflex) and polymer-on-metal type (e.g. SB Charite III, Prodisc L, Mobidisc, Activ-L) [5-8]. There are different models of total artificial discs, but one of the most popular involves a ball-and-socket design [3,4,6-9], as shown in Fig. 1. These current total prostheses do not mimic the static mechanical behaviour and the complex viscoelastic performance of the natural intervertebral disc. The scientific progresses made in the field of artificial intervertebral discs have involved hydrogel-based materials and multi-component fiber-reinforced hydrogel-based materials as nucleus replacement [15,17].

Mechanical and tribological behaviour of total prosthetic devices for human joints is still a major concern of national and international experts in the field of bioengineering, biomaterials, (bio) tribology and orthopaedics. In particular, total lumbar disc prosthesis has been very poorly studied from mechanical and tribological point of view; the most studied device was total hip prosthesis followed by the total knees prosthesis [3-7].

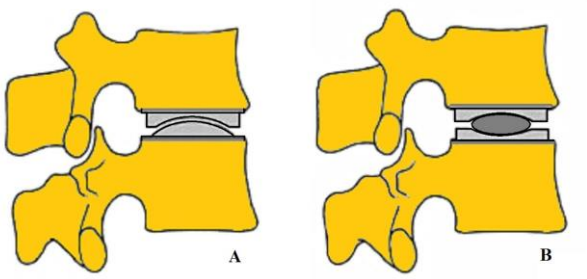


*Fig. 1. Ball-and-socket design for total disc prostheses on lumbar spine: A – artificial disc with two endplates; B – artificial disc with two concave endplates and a biconvex prosthetic nucleus.*

Prosthetic devices for lumbar disc are susceptible to functional improvements, especially in terms of more efficient use of biomaterials and more adequate design so as to give long-term functionality as close to healthy disc. The main requirements imposed on a lumbar disc prosthetic device are [13-25]:

- materials used in their manufacture must have properties of biocompatibility, durability and adequate mechanical properties;
- the prosthesis design must ensure a kinematic as close to natural disc in order to allow the physiological movements of the spine in flexion, extension, lateral bending and axial rotation;
- the prosthesis must permit the fixation to adjacent vertebrae;
- the artificial disc must ensure a durability at least 40 years.

The objective of this paper was to investigate theoretically the influence of ball radius on the maximum pressure and on the frictional torque which occurs within lumbar total disc prostheses made of different biomaterial combination. It was considered ball radii of *8-18 mm* and a radial clearance between ball and socket of *0.05 mm*. The maximum pressure and the frictional torque were then determined for different ball radii and for different biomaterial combinations as metal-on-metal, polymer-on-metal and ceramic-on-ceramic.

## 2. Materials and methods

### 2.1. Input parameters

Total disc prosthesis was considered to have a ball-and-socket design (Fig.1) with the ball having radii $R_1$ of *8, 10, 12, 14, 16* and *18 mm*, a radial clearance between ball and socket $c$ of *0.05 mm* and a socket radius $R_2 = R_1+c$. Surfaces in disc prosthesis have a very high conformity because of the very low radial clearance between the dimensions of endplates and prosthetic nucleus [11-13].

The biomaterial combinations considered in this study were CoCrMo-on-CoCrMo (Cobalt-Chromium-Molybdenum alloy), UHMWPE-on-CoCrMo (UHMWPE - ultra high molecular weight polyethylene) and $Al_2O_3$-on-$Al_2O_3$ (alumina ceramics). The mechanical properties for each biomaterial were listed in Table 1.

*Table 1. Mechanical properties of biomaterials: Young's modulus E and Poisson's ratio v [12,26]*

| Biomaterial | Young's modulus (GPa) | Poisson's ratio |
|---|---|---|
| CoCrMo | 210 | 0.3 |
| UHMWPE | 1 | 0.4 |
| $Al_2O_3$ | 392 | 0.29 |

As in many papers concerning the ball-and-socket geometry, an equivalent ball-on-plane configuration is adopted, simply defined by the equivalent radius $R_x$ and equivalent modulus of elasticity $E^*$ [12-14, 26-27]:

$$R_x = \frac{R_1 \cdot R_2}{R_2 - R_1} = \frac{R_1 \cdot (R_1 + c)}{c} \tag{1}$$

$$\frac{1}{E^*} = \frac{1}{2} \cdot \left( \frac{1-\nu_1^2}{E_1} + \frac{1-\nu_2^2}{E_2} \right) \tag{2}$$

The values of equivalent elastic modulus and friction coefficient for the three different biomaterial combinations were displayed in Table 2. In this study, for ceramic-on-ceramic combination it was considered an average friction coefficient of 0.036 [13]. In all cases the load was considered to be 200 N.

*Table 2. Biomaterial combinations, equivalent elastic moduli $E^*$ and friction coefficients μ*

| Couple of materials | Equivalent elastic modulus (GPa) [12] | Coefficient of friction [28] |
|---|---|---|
| CoCrMo-on-CoCrMo | 230.8 | 0.25 |
| UHMWPE-on-CoCrMo | 2.369 | 0.07 |
| $Al_2O_3$-on-$Al_2O_3$ | 428 | 0.002-0.07 |

### 2.2. Maximum pressure and frictional torque

The maximum pressure which occurs within total disc prostheses could be calculated with the following formula [13]:

$$p_0 = \frac{3 \cdot F_n}{2 \cdot \pi \cdot a^2} \tag{3}$$

where: $F_n$ is the normal force and $a$ is the semi-axis of Hertzian contact ellipse.

In ball-on-plane model the contact ellipse is a circle and in this special case the major semi-axis and minor semi-axis of the contact area are the same with the circle radius. Semi-axis of contact ellipse is given by:

$$a = \sqrt[3]{\frac{3 \cdot F_n}{E^* \cdot \sum \rho}} \tag{4}$$

where $\Sigma\rho$ is the curvatures sum and is defined by:

$$\sum \rho = 2 \cdot \left( \frac{1}{R_1} - \frac{1}{R_1 + c} \right) \tag{5}$$

According to the Fig. 2, when the ball has a small rotation motion around *X-axis* (to simulate flexion-extension motion of the lumbar spine), the elementary frictional torque $dM_f$, developed on the elementary contact

area $dA = 2 \cdot l(x) \cdot dx$, could be determined from the following equation [13]:

$$dM_f = \mu \cdot dF_n \cdot r(x) \tag{6}$$

where $\mu$ represents the friction coefficient.

The elementary normal force $dF_n$ is given by the equation:

$$dF_n = \frac{2}{3} \cdot p_0 \cdot \sqrt{1-\left(\frac{x}{a}\right)^2} \cdot 2l(x) \cdot dx \tag{7}$$

where:

$$r(x) = \sqrt{R_1^2 - x^2} \tag{8}$$

and

$$l(x) = \sqrt{a^2 - x^2} \tag{9}$$

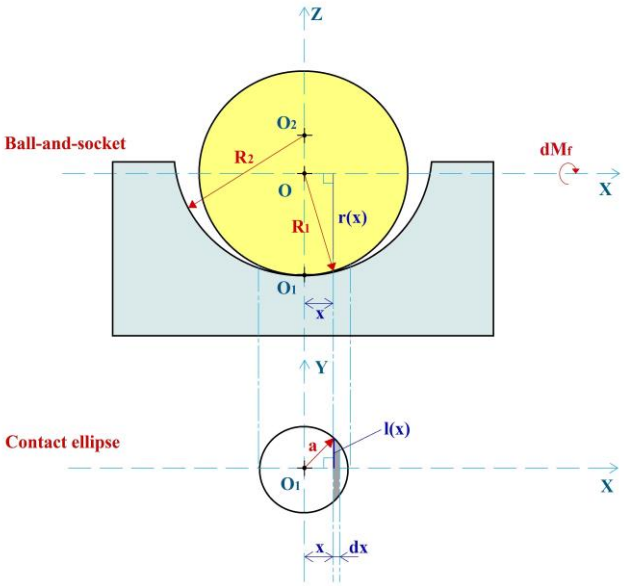


*Fig. 2. Ball-and-socket model and contact ellipse for total disc arthroplasty*

The following equation results from equations (6)-(9):

$$dM_f = \mu \cdot \frac{2}{3} \cdot p_0 \cdot \sqrt{1-\left(\frac{x}{a}\right)^2} \cdot 2\sqrt{a^2 - x^2} \cdot \sqrt{R_1^2 - x^2} \cdot dx \tag{10}$$

Consequently, the total frictional torque $M_f$ is given by the equation:

$$M_f = 4\int_0^a \mu \cdot \frac{F_n}{\pi \cdot a^2} \cdot \sqrt{1-\left(\frac{x}{a}\right)^2} \cdot \sqrt{a^2 - x^2} \cdot \sqrt{R_1^2 - x^2} \cdot dx \tag{11}$$

Another more complex method for determination of the frictional torque within the ball-and-socket design, after Houpert [29], is by taking into account the *X* and *Y* axes and the two semi-axes of the contact ellipse, *a* and *b* (Fig. 3).

Considering the two semi-axes of the contact ellipse, the maximum pressure is calculated with the following formula:

$$p_0 = \frac{3 \cdot F_n}{2 \cdot \pi \cdot a \cdot b} \tag{12}$$

The local pressure is calculated using the formula:

$$p(x,y) = p_0 \cdot \sqrt{1-\left(\frac{x}{b}\right)^2 - \left(\frac{y}{a}\right)^2} \tag{13}$$

The pressure on a half slice with the length $b_1$ located on *Y* axis [29] can be calculated with (Fig. 3):

$$p(x,y) = p_0 \cdot \sqrt{1-\left(\frac{x}{b}\right)^2 - \left(\frac{y}{a}\right)^2} = p_0 \cdot \sqrt{\left(1-\left(\frac{y}{a}\right)^2\right) \cdot \left(1-\left(\frac{x}{b_1}\right)^2\right)} = p(y) \cdot \sqrt{1-\left(\frac{x}{b_1}\right)^2} \tag{14}$$

where $p(y) = p_0 \cdot \sqrt{1-\left(\frac{y}{a}\right)^2}$ and $b_1 = b\sqrt{1-\left(\frac{y}{a}\right)^2}$.

The elementary frictional torque on this slice located on *Y* can be calculated with:

$$dM_f(y) = dF_f(y) \cdot r(y) \tag{15}$$

where: $r(y)$ is the lever arm defined by: $r(y) = \sqrt{R_1^2 - y^2}$ and $dF_f(y)$ is the elementary friction force on the slice $b_1$ [29]:

$$dF_f(y) = 2\int_0^{b_1} \mu \cdot p(x,y) \cdot dx = 2\mu \cdot p(y) \cdot \left[\int_0^{b_1} \sqrt{1-\left(\frac{x}{b_1}\right)^2} \cdot dx\right] \cdot dy \tag{16}$$

Finally, the elementary frictional torque on the slice $b_1$ is given by:

$$dM_f(y) = 2\mu \cdot p(y) \cdot r(y) \cdot \left[\int_0^{b_1} \sqrt{1-\left(\frac{x}{b_1}\right)^2} \cdot dx\right] \cdot dy \tag{17}$$

After the integration of equation (17), the total friction torque is:

$$M_f(y) = 6\mu \cdot \frac{F_n}{\pi \cdot a \cdot b} \cdot \int_0^a \sqrt{1-\left(\frac{y}{a}\right)^2} \cdot \sqrt{R_1^2 - y^2} \cdot \left[\int_0^{b_1} \sqrt{1-\left(\frac{x}{b_1}\right)^2} \cdot dx\right] \cdot dy \quad (18)$$

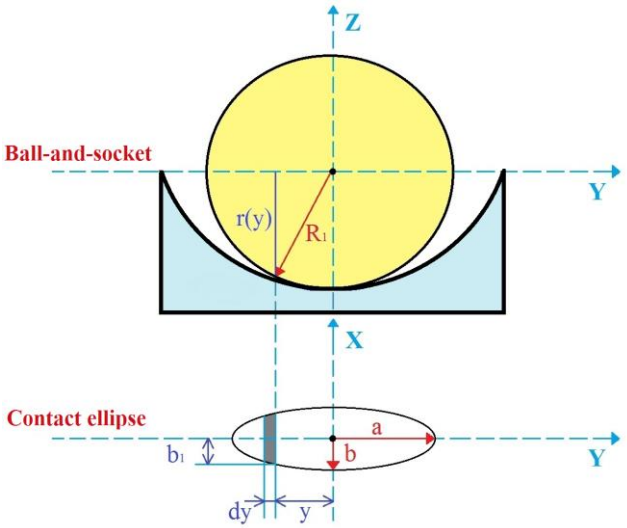


*Fig. 3. Ball-and-socket configuration and contact ellipse on axes X and Y*

## 3. Results and discussion

In order to study the influence of ball radius on the maximum pressure and on the frictional torque which occur within total disc arthroplasty devices for lumbar spine, the input parameters and equations have been introduced in Mathcad 14 software. The results about the effect of ball radius can be seen in Fig. 4 and Fig. 5. These results have indicated that increasing the ball radius decreased the maximum pressure (Fig. 4) and increased the frictional torque (Fig. 5).

Also, it can be seen that prosthesis with polyethylene-on-metal biomaterial combination has indicated low values of maximum pressure due to high levels of contact deformation; on the other hand, prostheses with metal-on-metal and ceramic-on-ceramic combination have indicated greater values, as it was observed in another study [13]. As expected, a greater equivalent elastic modulus has led to a reduced semi-axis of contact ellipse which has resulted in a greater maximum pressure. Therefore, maximum pressure values ranged from:

- (*67.7* to *23*) *MPa* for the biomaterial combination CoCrMo-on-CoCrMo (blue line of Fig. 4);
- (*3.2* to *1.1*) *MPa* for UHMWPE-on-CoCrMo (red line of Fig. 4);
- (*102.2* to *34.8*) *MPa* for $Al_2O_3$-on-$Al_2O_3$ (green line of Fig. 4).

It can be mentioned that in both metal-on-metal and ceramic-on-ceramic prostheses the semi-axis of contact area is much smaller than ball radius $R_1$, but this does not happen in case of polymer-on-metal couple (Table 3); for example, if the ball radius $R_1$ is considered of *14 mm* (and radial clearance *c* of *0.05 mm*), the semi-axis of contact ellipse will be more than *14 mm* under loads over *1102 N* (Table 4). The loads for polymer-on-metal devices when semi-axis of contact ellipse is more than ball radius were listed in Table 4. Therefore, the assumption of semi-infinite space and the use of an equivalent ball-on-plane geometry are justified only for hard-on-hard prostheses, after the reference [27].

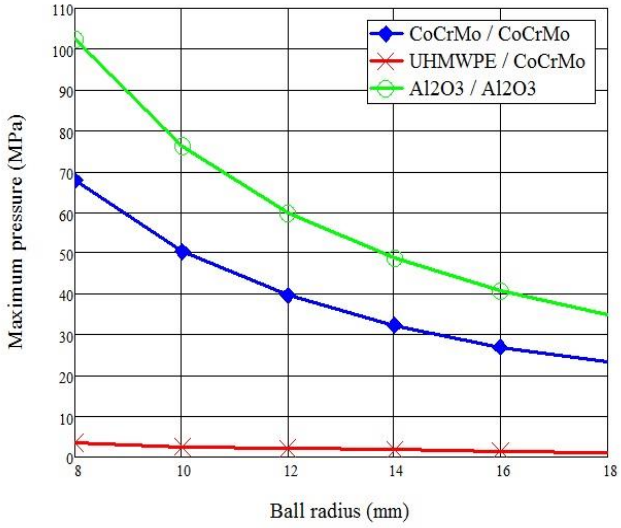


*Fig. 4. Variation in maximum pressure with ball radius $R_1$ under a load of 200 N*

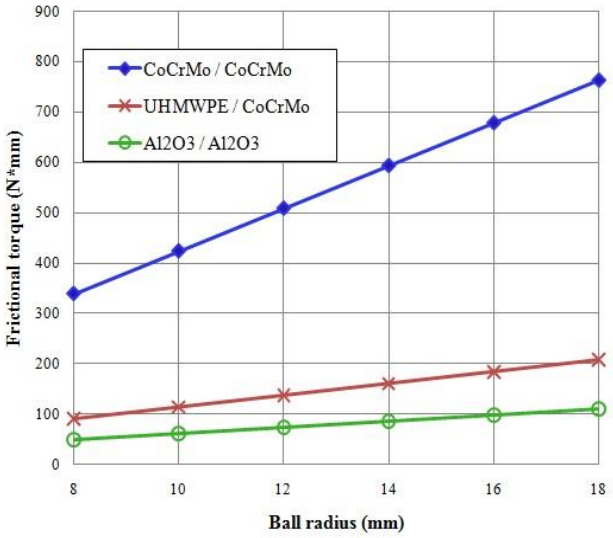


*Fig. 5. Variation in frictional torque with ball radius $R_1$ under a load of 200 N*

The influence of ball radius on the frictional torque for the three biomaterial combinations is shown in Fig. 5. It can be seen that increasing the ball radius has increased linearly the frictional torque. The highest values of frictional torque were detected in metal-on-metal combination and the lowest in polymer-on-metal and

ceramic-on-ceramic combinations, as it was shown in another study [13].

*Table 3. Comparison of semi-axes of contact ellipse and maximum pressures under loads of 200 and 2000 N*

| | $F_n$ = 200 N | | $F_n$ = 2000 N | |
|---|---|---|---|---|
| **Material combination** ($R_1$ = 14 mm, $c$ = 0.05 mm) | $a$ (mm) | $p_0$ (MPa) | $a$ (mm) | $p_0$ (MPa) |
| Metal-on-metal | 1.723 | 32.173 | 3.712 | 69.315 |
| Polymer-on-metal | 7.927 | 1.520 | 17.079 | 3.274 |
| Ceramic-on-ceramic | 1.402 | 48.562 | 3.021 | 104.624 |

*Table 4. Load values for polymer-on-metal devices when semi-axis of contact ellipse exceeds the ball radius*

| Ball radius $R_1$ (mm) | $F_n$ (N) for $a > R_1$ |
|---|---|
| 8 | ≥ 628 |
| 10 | ≥ 786 |
| 12 | ≥ 944 |
| 14 | ≥ 1102 |
| 16 | ≥ 1260 |
| 18 | ≥ 1418 |

This decreasing sequence of the frictional torque could be correlated with the friction coefficients of *0.25, 0.07* and *0.036*. Friction torque values ranged between:

- (*338.8* to *762.9*) *N·mm* for the biomaterial combination CoCrMo-on-CoCrMo (blue line of Fig. 5)
- (*90.4* to *207.9*) *N·mm* for UHMWPE-on-CoCrMo (red line of Fig. 5);
- (*48.8* to *109.9*) *N·mm* for $Al_2O_3$-on-$Al_2O_3$ (green line of Fig. 5).

Figs. 6 - 8 show the pressure distributions and contact ellipses for the three biomaterial combinations, under a load of *200 N* and for a socket radius of *14.05 mm*. It is noted that a lower contact ellipse has led to a higher maximum pressure. The higher maximum pressure has been recorded for ceramic-on-ceramic combination (Fig. 8).

In Fig. 9, the theoretical results from this study were compared with the results obtained using the Houpert method: the equation (18). It is noted that the values of friction torque using the Houpert method are more close to our results when the friction coefficient between the materials is lower (as in case of ceramic-on-ceramic). In case of metal-on-metal combination, it has been discovered a significant difference: between *60 N·mm* and *136 N·mm*.

A recent study realised by Moghadas et al. [11] has examined the friction in metal-on-metal disc prosthesis and showed that the frictional torque increases with load and also with ball radius. In that study the authors have performed frictional torque tests in new born calf serum, using a spine simulator, under loads of *50, 600, 1200* and *2000 N*. The prosthesis model used was metal-on-metal with ball radii spanning from *10* to *16 mm* and a radial clearance for ball-and-socket of *0.015 mm*.

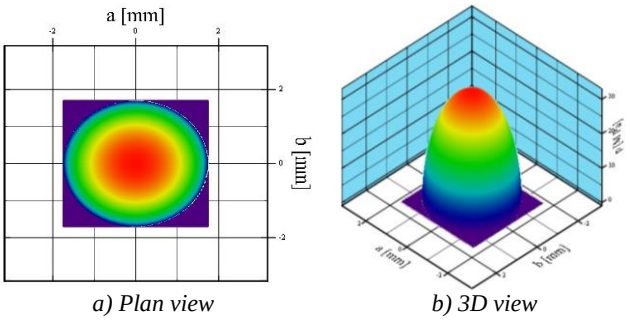


*a) Plan view* *b) 3D view*

*Fig. 6. Pressure distribution and contact ellipse for the biomaterial combination **metal-on-metal**, under a load of 200 N and a socket radius of 14.05 mm (a = b = 1.723 mm and $p_0$ = 32.17 MPa)*

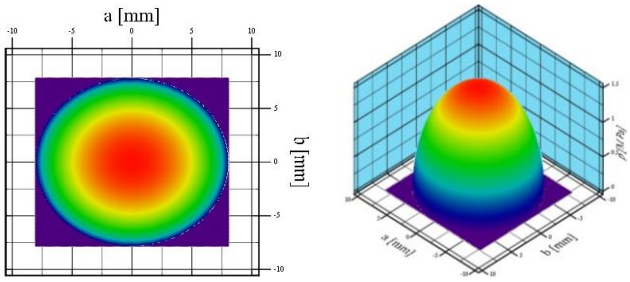


*a) Plan view* *b) 3D view*

*Fig. 7. Pressure distribution and contact ellipse for the biomaterial combination **polyethylene-on-metal**, under a load of 200 N and a socket radius of 14.05 mm (a = b = 7.928 mm and $p_0$ = 1.519 MPa)*

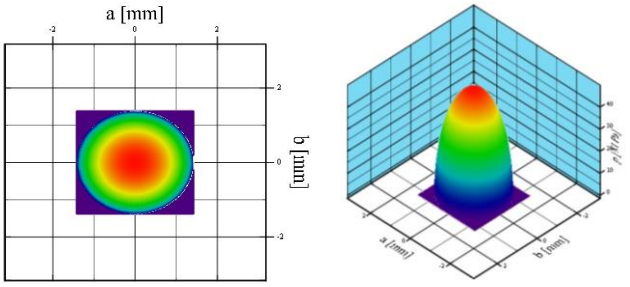


*a) Plan view* *b) 3D view*

*Fig. 8. Pressure distribution and contact ellipse for the biomaterial combination **ceramic-on-ceramic**, under a load of 200 N and a socket radius of 14.05 mm (a = b = 1.402 mm and $p_0$ = 48.562 MPa)*

The theoretical results of the frictional torque for metal-on-metal prosthesis type from this work can be validated with experimental results obtained by Moghadas et al. [11]. In this sense, the ball-and-socket model with ball radii of *10, 12, 14* and *16 mm* and a radial clearance of *0.015 mm* has been considered under loads of [11]:

a) $F_{n1}$ = *600 N*, with an average coefficient of friction $\mu_1$ of *0.8* (red line of Fig. 10);

b) $F_{n2}$ = *1200 N*, $\mu_2$ = *0.45* (green line of Fig. 10);

c) $F_{n3} = 2000$ *N*, $\mu_3 = 0.31$ (blue line of Fig. 10).

Fig. 10 shows the frictional torque against ball radius in both cases - theoretical and experimental - under different loads. The average coefficients of friction used for validation were taken from Stribeck curves presented in [11].

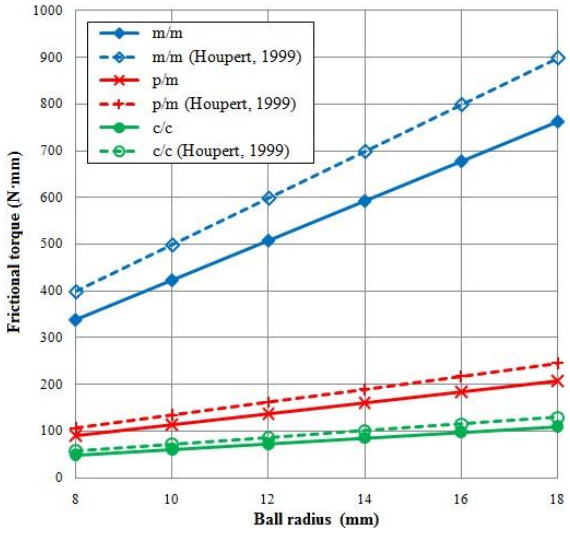


*Fig. 9. Validation of theoretical results for devices with different biomaterial combinations (m, p and c denote metal, polyethylene and ceramic, respectively)*

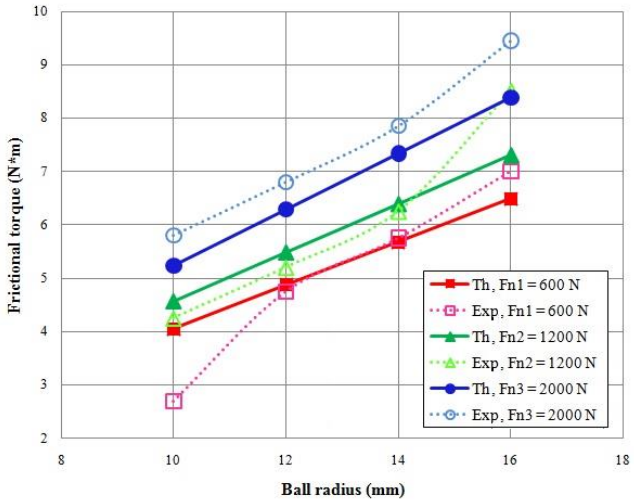


*Fig. 10. Variation in frictional torque with ball radius for metal-on-metal devices under the loads of 600, 1200 and 2000 N. Comparison of theoretical results with the experimental results from Moghadas et al. [11]*

It is noted that the theoretical values from numerical analysis have been found to be of the same order as those found in experimental tests. The differences between them could be caused by the approximation of average frictional torques for each ball radius and also by the approximation of average friction coefficients for each load, both from paper of Moghadas et al [11]. Moreover, this comparison of theoretical and experimental data has taken into account from experimental tests only the average frictional torques; but the authors [11] had found more close values of frictional torque for each ball radius and thereby they have demonstrated a significant linear correlation between frictional torque and radius, similar to numerical analysis (Fig. 5).

In this work, the theoretical estimations of maximum pressure and frictional torque depending on the ball radius have been done only in dry conditions, while within implanted total disc prosthesis the lubricant is represented by the interstitial fluid which have a viscosity of *1.24 mPa·s* [12-13]. In authors' opinion, the existence of interstitial fluid in biological environment could reduce the values of pressure and frictional torque from an implanted ball-and-socket lumbar prosthesis. The experimental data from [11] were obtained using new born calf serum and, as a result, the friction experimental values for loads lower than *2000 N* (Fig. 10) were lower than those predicted by the theoretical model.

Other studies on frictional torque in metal-on-metal hip prosthesis denoted similar results: by reducing the ball diameter, the friction is reduced due to the reduction of contact area [30] and metal-on-metal bearing surfaces shown a higher friction torque than that found for polymer-on-metal [31]. One study which investigated the effect of surface conformity on disc prosthetic devices showed that the increasing of socket radius (and therefore conformity factor) increased the maximum pressure and in a lesser extent, the frictional torque [13]. Another study which evaluated the stress in total disc prosthesis for lumbar spine using finite element method indicated that hard-on-hard material combination has higher values of stress distribution than soft-on-hard couple [10].

## 4. Conclusions

Total disc prostheses are becoming increasingly popular in many countries and that is why more studies on the biomaterial tribological performance of these devices are required. The most common design of these prostheses is ball-and-socket. This paper has investigated theoretically the effect of ball radius on the maximum pressure and on the frictional torque that occur in total disc prostheses for lumbar spine made of different biomaterials. Therefore, the maximum pressure has been found to decrease with ball radius, while the frictional torque has increased linearly with ball radius for each biomaterial combination. The lowest values of frictional torque have been detected in ceramic-on-ceramic. In order to reduce friction, this study has suggested designing of total disc prostheses for lumbar spine with small ball radius and with ceramic-on-ceramic bearing surfaces.

**Acknowledgements**

This paper was realised with the support of POSDRU CUANTUMDOC "DOCTORAL STUDIES FOR EUROPEAN PERFORMANCES IN RESEARCH AND INNOVATION" ID79407 project funded by the European Social Fund and Romanian Government.

## References


[1] C.D. Ray, Spine **22**, 667 (1997).
[2] A. Gloria, L. Manto, R. De Santis, L. Ambrosio, J Appl Biomater Biomech **6**, 163 (2008).
[3] S. Gravius, M. Weisskopf, J. A. K. Ohnsorge, U. Maus, F. U. Niethard, D. C. Wirtz, Dtsch Arztebl **104**(38), A2592 (2007).
[4] D. P. Sakalkale, S. A. Bhagia, C. W. Slipman, Pain Physician **6**(2), 195 (2003).
[5] G. Denoziere, D. N. Ku, J Biomech **39**, 766 (2006).
[6] I. Rotaru, F. Munteanu, D. Olaru, Mecatronica, Ed. SROMECA **1**, 9 (2011), ISSN 1583-7653.
[7] T. F. Fekete, F. Porchet, Acta Neurochir **152**, 393 (2010).
[8] T. Zander, A. Rohlmann, G. Bergmann, Clin Biomech **24**, 135 (2009).
[9] K. D. van den Eerenbeemt, R. W. Ostelo, B. J. van Royen, W. C. Peul, M. W. van Tulder, Eur Spine J **19**, 1262 (2010).
[10] I. Rotaru, F. Munteanu, D. Olaru, Proc. 3-rd IEEE Intern. Conf. EHB, Ed. "Gr.T.Popa" University of Medicine and Pharmacy of Iasi, Romania, 2011, p. 211.
[11] P. Moghadas, A. Mahomed, D. W. L. Hukins, D. E. T. Shepherd, J Biomech **45**, 504 (2012).
[12] A. Shaheen, D. E. T. Shepherd, J Eng Med **221**, H 621 (2007).
[13] I. Rotaru, D. Olaru, Bulletin of the Polytechnic Institute of Iasi, t. LVIII (LXII) **2**, 147 (2012).
[14] I. Rotaru, D. Olaru, Bulletin of the Polytechnic Institute of Iasi, t. LVIII (LXII) **2**, 137 (2012).
[15] A. Gloria, R. De Santis, L. Ambrosio, F. Causa, K. E. Tanner, J Biomater Appl **25**, 795 (2011).
[16] I. Rotaru, B. Istrate, M. Benchea, A. Tufescu, D. Olaru, TEHNOMUS, 112, (2013).
[17] S. Reitmaier, U. Wolfram, A. Ignatius, H. J. Wilke, A. Gloria, J. M. Martín-Martínez, J. Silva-Correia, J. M. Oliveira, R. L. Reis, H. Schmidt, J Mech Behav Biomed Mater **14**, 67 (2012).
[18] H. Serhan, D. Mhatre, H. Defossez, C. M. Bono, SAS Journal **5**, 75 (2011).
[19] J. L. Tipper, P. J. Firkins, A. A. Besong, P. S. M. Barbour, J. Nevelos, M. H. Stone, E. Ingham, J. Fisher, Wear **250**, 120 (2001).
[20] W. Wang, H. Zhang, K. Sadeghipour, G. Baran, Med Eng Phys **35**, 357 (2013).
[21] S. H. Chen, Z. C. Zhong, C. S. Chen, W. J. Chen, C. Hung, Med Eng Phys **31**, 244 (2009).
[22] M. Bushelow, W. Nechtow, J. Walker, The 23-rd Annual Meeting of the North American Spine Society, P8 (2008).
[23] T. M. Grupp, J. J. Yue, R. Garcia, J. Basson, J. Schwiesau, B. Fritz, W. Blomer, Eur Spine J **18**, 98 (2009).
[24] W. Nechtow, W. Long, D. Coombs, M. Bushelow, M. Hintner, A. Ochs, C. Kaddick, The 54-th Annual meeting of the Orthopaedic Research Society, 1928 (2008).
[25] G. Pop, Biomateriale si componente protetice metalice, Ed. Tehnopress, Iasi, (2004).
[26] T. Pylos, D. E. T. Sheperd, J Biomech **37**, 405 (2004).
[27] L. Matei, F. Di Puccio, B. Piccigallo, E. Ciulli, Tribol Int **44**, 532 (2011).
[28] D. Kopeliovich, Materials for joint prostheses; accessed on May 2011 from URL: http://www.substech.com .
[29] L. Houpert, Congres Roulement, Toulouse, May 5-7 (1999).
[30] R. M. Streicher, M. Semlitsch, R. Schon, H. Weber, C. Rieker, Proc. of the Institution of Mechanical Engineering, Part H – J Eng Med **210**, 223 (1996).
[31] N. E. Bishop, F. Waldow, M. M. Morlock, Med Eng Phys **30**, 1057 (2008).



*Corresponding author: rotaruiuliana2000@gmail.com
rotaruiuliana@tuiasi.ro